

Non-Stationary Motor Fault Detection Using Recent Quadratic Time-Frequency Representations

Satish Rajagopalan Thomas G. Habetler
Ronald G. Harley
School of Electrical and Computer Engineering
Georgia Institute of Technology
Atlanta GA 30332-0250 USA
thabetler@ece.gatech.edu

José A. Restrepo José M. Aller
Universidad Simón Bolívar
Caracas 1080A, VENEZUELA
restrepo@usb.ve

Abstract — Fault detection in electric motors operating under non-stationary operating conditions has been gaining importance, due to the fact that motors are used in many applications such as actuators in the aerospace and transportation industries operate under conditions that rapidly vary with time. In recent times, a plethora of new time-frequency distributions have appeared that are inherently suited to the analysis of non-stationary signals while offering superior frequency resolution characteristics. The Zhao-Atlas-Marks (ZAM) distribution is one such distribution. This paper proposes the use of these new time-frequency distributions to enhance non-stationary fault diagnostics in electric motors. One common myth has been that the quadratic time-frequency distributions are not suitable for commercial implementation. This paper addresses this issue in detail too. Optimal discrete time implementations of some of these quadratic time-frequency distributions are explained. These TFRs have been implemented on a digital signal processing (DSP) platform to demonstrate that the proposed methods can be implemented commercially.

Keywords- *Electric machines, condition-monitoring, eccentricity, ZAM, CWD, time-frequency distributions, rotor faults*

I. INTRODUCTION

Fault detection in electric motors operating under non-stationary operating conditions has been gaining importance in recent times, due to the fact that motors used in most applications such as actuators in the aerospace and transportation industries operate under conditions that rapidly vary with time. Several non-stationary signal analysis techniques have been applied to track fault signatures in the stator current of motors operating in such transient conditions [1, 2]. The short time Fourier transform (STFT), a linear time-frequency representation (TFR), is one such technique that has been widely used due to its robustness and simplicity [1, 2]. The STFT is however dependent on the type and length of the window as it has to be chosen as a trade off between time and frequency resolution. Quadratic TFRs have been recently proposed as an alternative to STFT due to their independence from the choice or size of the window and their inherent suitability to non-stationary signals. The Wigner-Ville distribution (WVD) and its variants, especially the smoothed pseudo Wigner-Ville distribution (SPWVD) has been suggested as a possible choice [3]. However, these

distributions come with their own drawbacks, namely, the introduction of non-negligible cross-term artifacts in the time-frequency spectrum. These artifacts can often suppress the fault frequencies that are produced in the current signal. Improved distributions such as the Choi-Williams distribution (CWD) have shown reduction in cross-term artifacts at the cost of loss in frequency resolution [4].

However, in recent times there has been a plethora of new time-frequency distributions that provide strong cross-term suppression while offering superior frequency resolution characteristics. The Zhao-Atlas-Marks (ZAM) distribution is one such distribution [5]. There have also been new techniques to improve the readability of traditional quadratic time-frequency distributions such as the reassigned SPWVD. While [2, 3] investigated the use of time-frequency distributions in BLDC rotor fault detection under continuously changing motor operating conditions, this paper expands the subject by exploring the use of newer and more recently developed time-frequency distributions to enhance non-stationary fault diagnostics in electric motors. One common myth has been that the quadratic time-frequency distributions are not suitable for commercial implementation. This paper addresses this issue in detail too. Optimal discrete time implementations of some of these quadratic time-frequency distributions will be explained. These TFRs have been implemented on a digital signal processing (DSP) platform to demonstrate that the proposed methods can be implemented commercially.

II. QUADRATIC TIME-FREQUENCY REPRESENTATIONS FOR NON-STATIONARY BLDC MOTOR FAULT DIAGNOSTICS

Time-frequency analysis is the three-dimensional time, frequency, and amplitude representation of a signal, which is inherently suited to indicate transient events in a signal. In 1966, Cohen developed a generalized form of phase-space distribution from which all other time-frequency distributions could be derived. These distributions are essentially energy distributions as they distribute the energy of the signal over the two description variables: time and frequency. As the energy is a quadratic function of the signal, the Cohen class time-frequency energy distributions are quadratic representations. These distributions can be used for the analysis of true non-stationary signals without any underlying assumptions. The

general form of the Cohen's class of distributions for a signal $f(t)$ is given by [6]

$$D(t, \omega, \varphi) = \iiint e^{j(\xi\mu - \tau\omega - \xi t)} \varphi(\xi, t) \cdot f\left(\mu + \frac{\tau}{2}\right) f^*\left(\mu - \frac{\tau}{2}\right) d\mu d\tau d\xi, \quad (1)$$

where $\varphi(\xi, \tau)$ is the transformation's kernel that defines the transformation. This equation can be re-written in terms of the Generalized Ambiguity function (GAF), $A(\xi, \tau; \varphi)$, [7] as

$$D(t, \omega, \varphi) = \frac{1}{4\pi^2} \iint A(t, \omega; \varphi) e^{-j(\xi t + \tau\omega)} d\xi d\tau, \quad (2)$$

where the GAF is described by the following expression.

$$A(\xi, t; \varphi) = \varphi(\xi, \tau) \int_{-\infty}^{\infty} f\left(\mu + \frac{\tau}{2}\right) f^*\left(\mu - \frac{\tau}{2}\right) e^{-j\xi\mu} d\mu \\ = \frac{\varphi(\xi, \tau)}{2\pi} \int_{-\infty}^{\infty} F\left(v + \frac{\xi}{2}\right) F^*\left(v - \frac{\xi}{2}\right) e^{jv\tau} dv \quad (3)$$

The duality between the Ambiguity function and the Wigner-Ville distribution (WVD) shown in [8] can be extended to the GTFD and the GAF. From the previous equations it can be seen that the GAF is the dual of the GTF in the sense of the Fourier transform. A property of interest is the one referring to the interference geometry. For a multi-component signal the elements of the GAF corresponding to auto-terms are mainly located around the origin, while the interference components or cross-terms are located away from the origin, at a distance proportional to the time-frequency distance between the auto-terms.

According to this, and since the time frequency structure of the current signal in a BLDC machine is changing, the best suited time frequency distribution is the one that selects a region around the origin in the ambiguity domain, and reduces to zero away of the origin. The distributions, also known as reduced interference distributions, dependant on the product of $\xi\psi$ and $\tau\psi$ provide this kind of selection. Examples of these distributions are the Choi-Williams distribution (CWD), the Born-Jordan distribution (BJ), and the Zhao-Atlas-Marks (ZAM) or cone-shaped distribution. The weighting function for these distributions is shown in figures 1(a), 1(b), and 1(c). As mentioned before, the spectral content of the BLDC stator current is changing, and although the reduced interference distributions produce good results, a better approach would be to use an adaptive optimal kernel [9]. The procedure is based on the adaptation of a radial Gaussian kernel over a short-time ambiguity function around the time instant of interest [9]. This procedure is computationally more demanding since it requires an additional adaptation step that fixed kernel distributions do not have. In any case the use of an adaptive kernel provides information over the relative quality of the results provided by the fixed kernel distributions.

III. TIME-FREQUENCY KERNELS IN DETAIL

Several reduced interference distributions have since been proposed, which are all a subset of the Cohen's class. Some of these distributions are Margenau-Hill, Kirkwood-Rihaczek, Born-Jordan (BJ), and the CWD [10]. The ZAM distribution is a relatively new distribution [5]. While the emphasis on development of distributions such as the CWD was to meet marginal conditions and other properties [10], the development of ZAM "cone-kernel" was intended to introduce finite time support and reduce cross-terms [5]. The kernel to be used in (1) to obtain a ZAM distribution is

$$\varphi(\xi, \tau) = \varphi_1(\tau) \frac{\sin(\xi|\tau|/a)}{\xi/2}, \quad (4)$$

where $\varphi_1(\tau)$ is a function to be specified (usually taken to be equal to one) and a is greater than or equal to two. The cone-shaped kernel function suppresses the cross terms away from the vertical axis and the origin of the ambiguity function plane. The BJ distribution is similar to the ZAM distribution. The ZAM distribution is nothing but a Born-Jordan distribution (5) with finite time support and smoothed along the frequency axis.

$$\varphi(\xi, \tau) = \frac{\sin(\xi\tau)}{\xi\tau/2}. \quad (5)$$

The exponential kernel function or the Choi-William kernel has the same dimensions as the ambiguity function. The exponential kernel function suppresses the cross terms away from the horizontal axis and the vertical axis. Therefore, the CWD reduces the cross terms generated by two auto terms with different time centers and frequency centers. The CWD has a coarser time-frequency resolution than the WVD because the CWD also blurs the auto terms when the CWD reduces the cross terms. The Choi-William exponential kernel is given as

$$\varphi(\xi, \tau) = e^{-\xi^2\tau^2/\sigma}, \quad (6)$$

where the parameter σ determines the trade-off between the cross-term suppression and the frequency resolution. If σ has a large value, then the kernel is effectively one and results in the WVD. A smaller σ on the other hand enhances the actual frequency components in the signal (also termed as auto-terms) while suppressing the cross terms.

IV. BLDC MOTOR FAULT DIAGNOSTICS USING QUADRATIC TIME-FREQUENCY REPRESENTATIONS (TFR)

Quadratic time-frequency distributions explained in the previous section are used in this research to extract non-stationary fault frequency signatures from the BLDC motor current using the well known "Motor current signature analysis (MCSA)" technique [11]. This technique is based on the fact that rotor faults such as dynamic eccentricity or unbalanced rotors produce unique characteristic fault frequency signatures in the motor current spectra. By way of an example, in BLDC

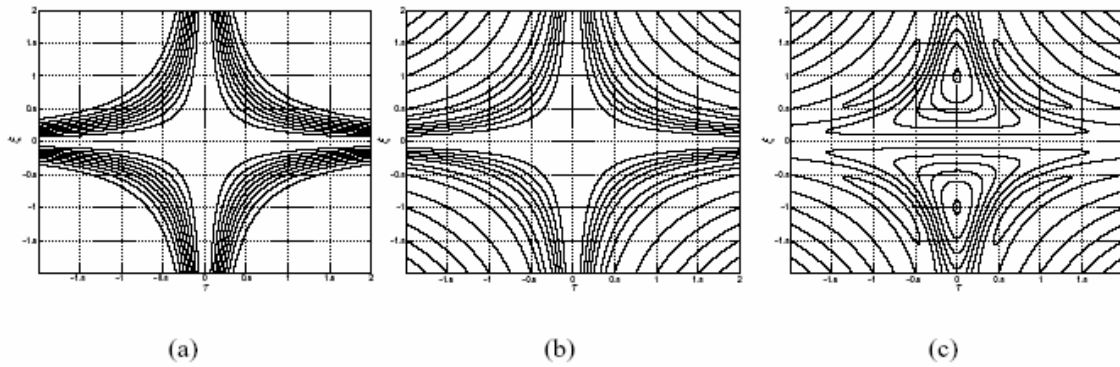


Figure 1. Weighting function for the (a) Choi-Williams distribution, (b) Born-Jordan distribution, (c) ZAM distribution.

motors operating at constant speed, the dynamic eccentricity fault frequencies are given by, [12]

$$f_{rf} = f_e \pm k \frac{f_e}{P/2}, \quad (7)$$

where, f_{rf} is the rotor fault frequency, f_e is the fundamental frequency, P is the number of poles in the BLDC machine, and k is any integer. These fault frequencies are also present when the current is in a non-stationary state and are tracked using the proposed quadratic TFR based detection algorithm shown in Fig. 2. The acquired BLDC stator current is first filtered adaptively to remove the fundamental frequency and other inverter harmonics. This selective adaptive filtering prevents cross-terms from being introduced at frequencies of interest. The filtered stator current is then converted into an analytic signal using a Hilbert transformation [2-3, 13]. The fault frequencies are then extracted from this analytic signal by computing the ZAM distribution (1, 2). Other TFRs such as the CWD can be used in place of the ZAM distribution if needed. A simple fault metric is then calculated by computing the root mean square (RMS) value of the instantaneous amplitudes of the extracted fault frequencies. This metric is used to indicate a developing rotor fault. Thresholds can be set to determine the severity of the fault and provide an indication to the operator to take some necessary precautionary action. The fault investigated in this paper is dynamic eccentricity, although the proposed technique can be extended to other faults such as unbalanced rotors, bearing defects, and broken rotor bars in induction motors.

V. BLDC MOTOR FAULT DIAGNOSTICS – EXPERIMENTAL AND SIMULATED RESULTS

A six-pole 12 V, 1 kW BLDC motor with speed and current control is used in the experiments. For a six-pole BLDC motor, the rotor fault frequencies occur at $1/3^{\text{rd}}$, $2/3^{\text{rd}}$, $4/3^{\text{rd}}$, and $5/3^{\text{rd}}$ times the fundamental frequency, as per (7). Figure 3 shows the spectrogram (short-time Fourier transform) of a simulated non-stationary motor current signal. Such a hypothetical signal has been explained in detail in [2]. It can also be seen from Fig. 3 that the spectral components produced by the spectrogram are smeared (or thick) in the frequency domain. Hence, the fault frequencies are not localized but spread over a frequency range. The BJ distribution of the

simulated rotor fault signal calculated using the Rice University t-f toolbox [8] is shown in Fig. 4. This toolbox has specific functions tailor made for time-frequency analysis. Even though the frequency resolution is very good (all the three frequencies are distinctly tracked), the distribution still suffers from cross-terms. The ZAM distribution in Fig. 5 on the other hand shows good energy concentration (low frequency smear), excellent cross-term suppression and much better frequency resolution than the spectrogram.

Experimental results are also obtained to demonstrate the viability of using the ZAM distribution as a tool for non-stationary motor fault detection. The speed reference of the BLDC motor is varied sinusoidally or in a triangular pattern to obtain non-stationary motor operation. A high attenuation (56 db) switch capacitor filter is used to adaptively filter out the fundamental and all harmonics that are larger than twice the fundamental frequency, from the BLDC stator current prior to data acquisition. The hardware setup for the non-stationary motor operation test including the implementation of the dynamic eccentricity is explained in detail in [2]. The same test set-up is used in this paper, with the speed reference of the BLDC motor drive varied in different non-stationary patterns. The Rice University t-f toolbox [8] is again used to calculate the time-frequency representations of the filtered BLDC current signal. Fig. 6 shows the ZAM distribution of the filtered stator current of a dynamically eccentric BLDC motor (32% dynamic air-gap eccentricity) now operating with a 5 Hz sinusoidal speed reference. Again, the ZAM distribution tracks the fault frequencies distinctly over time. The ZAM distribution's good frequency resolution, sharp energy concentration, and ability to handle non-stationary signals are an important advantage in fast non-stationary signals. To demonstrate this advantage, the ZAM distribution of the filtered stator current signal of the same dynamically eccentric BLDC motor (Fig. 7) operating with a 10 Hz triangular speed reference, is compared to the STFT of the same signal (Fig. 8). The STFT is computed using a Hamming window of size 0.25 seconds. This length is obtained through trial and error so as to obtain a good compromise between the time and frequency resolutions for this problem. The ZAM distribution distinctly tracks the fault frequencies in the filtered stator current. The energy concentration is sharp and the frequency resolution at low frequencies is better than that of the STFT, as shown in Fig. 8.

Figure 9 shows a simple fault metric calculated using the instantaneous root mean square value (RMS) of the fault frequency amplitudes extracted using the ZAM distribution from the filtered stator current of a good BLDC motor. This is also compared with the instantaneous RMS of the rotor fault frequencies extracted from a BLDC motor with dynamic eccentricity. In both these cases (Fig. 9), the BLDC motor is operating with a 5 Hz sinusoidal speed reference. An adaptive threshold that varies as a fixed percentage of the fundamental frequency component (in this case chosen as 2%) is used for automatic detection of rotor faults. The RMS fault metric of the defective BLDC motor is significantly different than the RMS fault metric of a good motor. Fig. 9 also shows that the adaptive threshold effectively discriminates the fault over time when compared to a good motor.

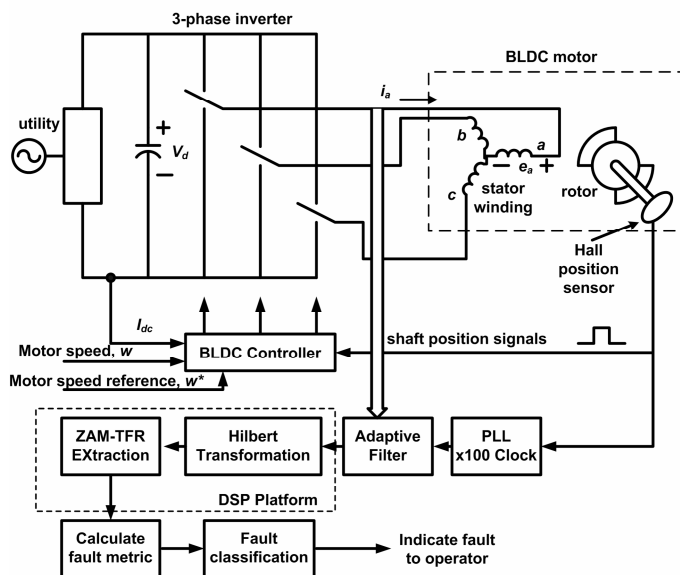


Figure 2. Rotor fault detection in BLDC motors using TFRs.

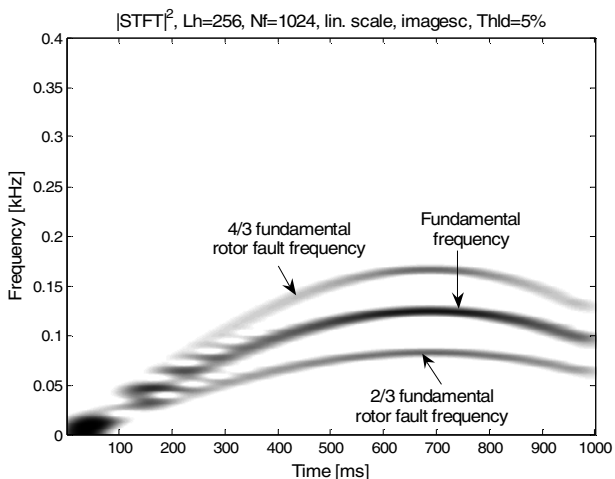


Figure 3. STFT of simulated BLDCM rotor fault comprising of three frequencies varying over time.

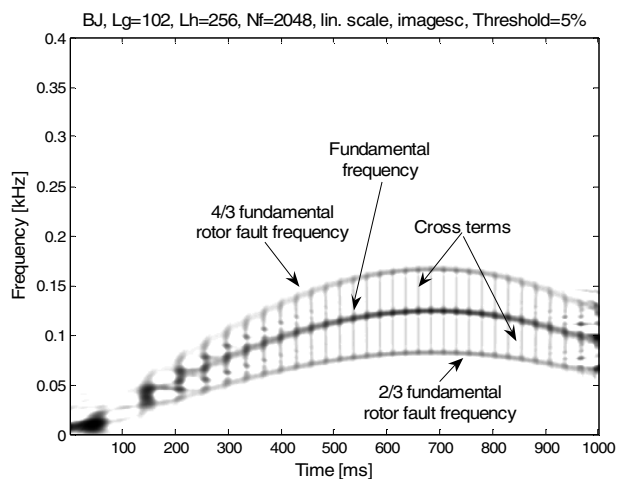


Figure 4. BJ of simulated BLDCM rotor fault comprising of three frequencies varying over time.

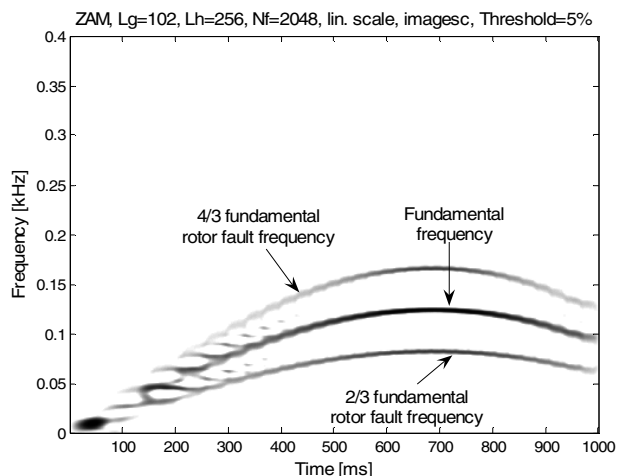


Figure 5. ZAM of simulated BLDCM rotor fault comprising of three frequencies varying over time.

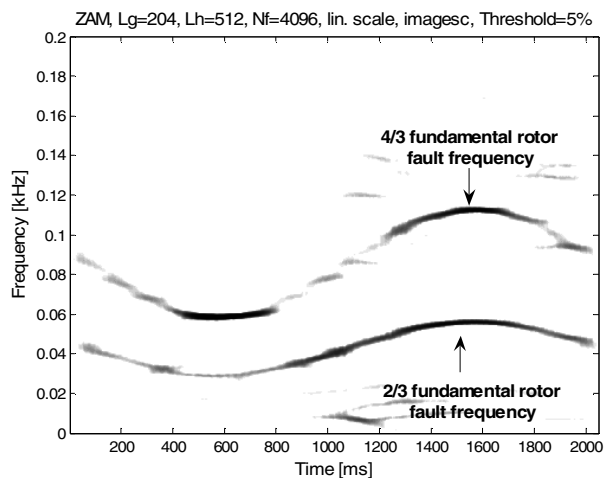


Figure 6. ZAM of filtered BLDC motor (with dynamic eccentricity) stator current and 5 Hz sinusoidal speed reference.

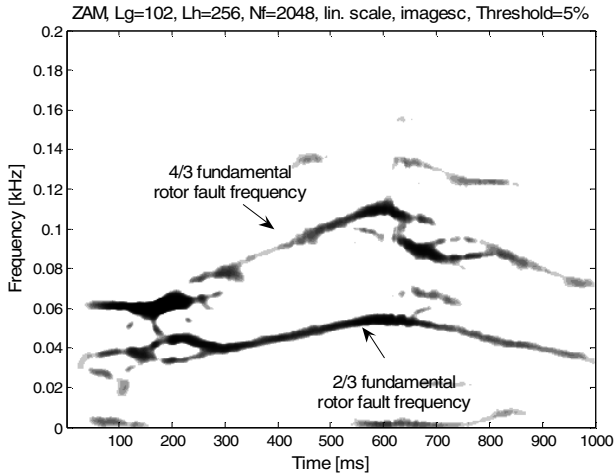


Figure 7. ZAM of filtered BLDC motor (with dynamic eccentricity) stator current and 10 Hz triangular speed reference.

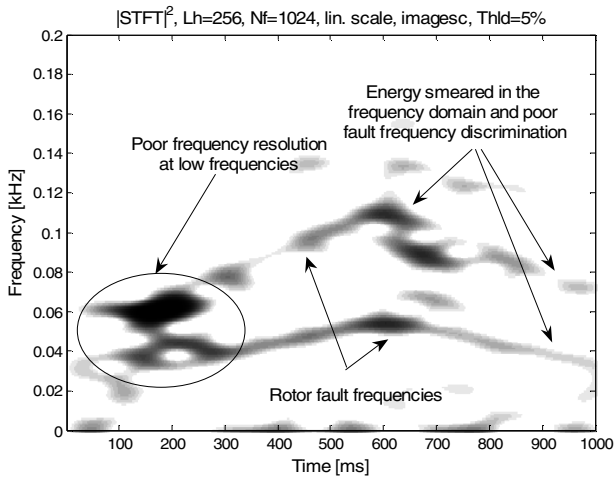


Figure 8. STFT of filtered BLDC motor (with dynamic eccentricity) stator current and 10 Hz triangular speed reference.

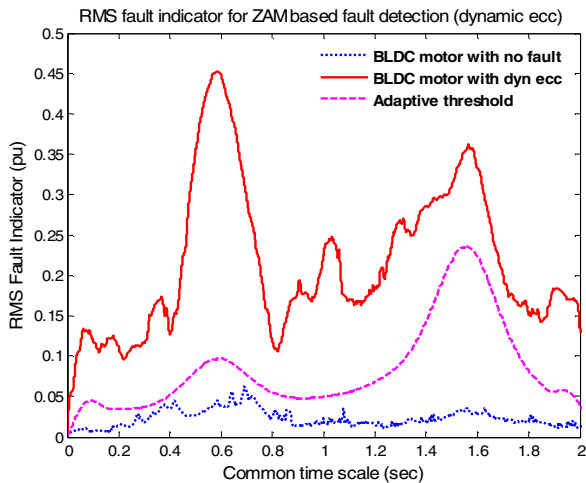


Figure 9. RMS fault indicator discriminates BLDC rotor eccentricity using an adaptive threshold (5 Hz sinusoidal speed ref).

VI. COMMERCIAL IMPLEMENTABILITY OF QUADRATIC TFRS FOR BLDC MOTOR FAULT DIAGNOSTICS

One common mistaken belief has been that the recent quadratic time-frequency representations (TFRs) are not suitable for commercial implementation due to their complexity. The TFRs are implemented on an ADSP21160-SHARC DSP operating with a 80 MHz clock and the time taken for computing one time slice of information is recorded using an oscilloscope.

For practical implementation of distributions members of Cohen's class, the generalized discrete-time discrete-frequency distribution (GDTDFD) is defined as [10]

$$\hat{P}(l, \theta; \hat{\Phi}) = \sum_{n=-\infty}^{+\infty} R_l(n) e^{-j2n\theta}, \quad (8)$$

where the auto-correlation sequence R_l is,

$$R_l(n) = \sum_{m=-\infty}^{+\infty} s(l+m+n) s^*(l+m-n) \hat{\Phi}(m, 2n) \quad (9)$$

$\hat{\Phi}(m, 2n)$ is the discrete-domain kernel that defines the time-frequency representation. In practice only a finite span in time of the signal is available. This can be represented by applying a sliding window to the signal under analysis, so that equations (8) and (9) can be rewritten as follows:

$$\hat{P}(l, \theta; \hat{\Phi}) = \sum_{n=-N}^{+N} R_l(n) e^{-j2n\theta} \quad (10)$$

and

$$R_l(n) = \sum_{m=-M}^{+M} s(l+m+n) s^*(l+m-n) \hat{\Phi}(m, 2n) \quad (11)$$

The auto-correlation sequence is first computed and the discrete Fourier transform (DFT) is computed to obtain the DWVD of the sequence. The DWVD can be efficiently computed using standard Fast Fourier transform (FFT) algorithms. The computation is further optimized by evaluating two successive R_l sequences together [14]:

$$R_{comb}^{WD} = R_{l1}(n) + j R_{l2}(n) \quad (12)$$

The discrete Fourier transform (DFT) of the individual sequences can be evaluated using a single DFT for the combined kernel, thus halving the number of final FFTs used. The Hilbert transform is implemented as a 79-tap FIR filter [14].

A. Implementation of ZAM, BJ and CW distributions.

The load computations for one time slice of data processed is measured on an oscilloscope and is compared in Table I for $N=M=64$ points. The ZAM distribution is compared with the BJ, CWD, and the STFT. The amount of computation in the ZAM algorithm, for a 64 points FFT and 64 points correlation windows is as follows: The correlation matrix update requires $(2*N=128)$ additions and $(4*N=256)$ products. The computation of the correlation vector requires $(2*N^2=8192)$

additions and ($2 \times N^2 = 8192$) products. The computationally intensive part of the algorithm, apart from the FFT, is the correlation computation. The actual algorithm implementation uses the same operations for different kernels (generic kernels). The results shown in Table 1 are obtained for an ADSP21160, 80 MHz board.

TABLE 1
COMPUTATION TIME QUADRATIC TFR KERNELS,
WITH $N=M=64$

TFR	Computation time per time slice (μ -sec)
Spectrogram	40
CW, BJ and ZAM	880

VII. REASSIGNED TIME-FREQUENCY DISTRIBUTIONS

Another method of further improving the performance of TFRs is the use of reassignment. In a reassigned SPWV, the computed values of a regular SPWV are moved to a different plane depending on the instantaneous frequency and time-delay [15]. The reassignment method automatically compresses the energy in the quadratic time-frequency representation toward the centers of gravity of the signal components to make the signal components more concentrated. Figure 10 shows the reassigned SPWV of a part of the motor stator current signal shown in Fig. 6 that shows much better frequency concentration than a regular TFR.

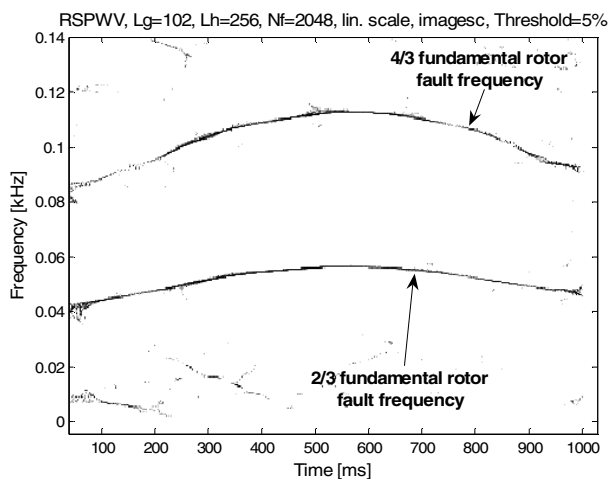


Figure 10. Reassigned SPWV of filtered BLDC motor (with dynamic eccentricity) stator current and 5 Hz sinusoidal speed reference.

VIII. CONCLUSIONS

This paper presents the use of new advances in non-stationary signal analysis, particularly quadratic time-frequency distributions, towards rotor fault detection in BLDC motors. Recent distributions such as the ZAM distribution offer superior performance when compared to traditional techniques such as the short-time Fourier transform. This is demonstrated

through both simulation and experimental results. The reason behind the good performance of these distributions is that they are designed with an emphasis on improved frequency/time resolution and cross term suppression, rather than to satisfy the marginal properties of a traditional t-f distribution.

The detection of dynamic eccentricity in BLDC motors is specifically illustrated in this paper as an example. However, the proposed method can be extended to detect other faults such as bearing faults, gear faults. The method can also be readily applied to faults in other kinds of motors such as broken rotor bar detection in induction motors.

A common belief is that these new distributions are too complicated to be implemented in a commercial system due to their intense computational time. To address this issue, the time-frequency distributions have been implemented on a DSP platform. While the computational time for these distributions is larger than for conventional techniques such as the short-time Fourier transform, they can still be efficiently used because motor condition monitoring is performed over long intervals of time. Hence, any condition monitoring technique is usually not a burden on the computational capability of the DSP.

ACKNOWLEDGMENT

The authors wish to acknowledge the support of Delphi Corp., Troy, MI, and in particular the help of Dr. Tomy Sebastian (Delphi Saginaw Steering Systems), and Drs. Bruno Lequesne and Thomas W. Nehl (Delphi Research Labs), as well as financial support from the Duke Power Company in Charlotte, North Carolina.

REFERENCES

- [1] B. Yazici and G. B. Kliman, "An adaptive statistical time-frequency method for detection of broken bars and bearing faults in motors using stator current," *IEEE Trans. Ind. Appl.*, vol.35, no. 2, pp. 442-452, 1999.
- [2] S. Rajagopalan, José M. Aller, José A. Restrepo, T.G. Habetler, and R.G. Harley, "Diagnosis of Rotor Faults in Brushless DC (BLDC) Motors Operating under Non-Stationary Conditions Using Windowed Fourier Ridges," in *Proc. 40th Annual Meeting of the Industry Applications Society (IAS 2005)*, 2005, pp. 26-33.
- [3] S. Rajagopalan, J. A. Restrepo, J. M. Aller, T. G. Habetler, and R. G. Harley, "Wigner-Ville Distributions for Detection of Rotor Faults in Brushless DC (BLDC) Motors Operating Under Non-Stationary Conditions," in *Proc. International Symposium on Diagnostics for Electric Machines, Power Electronics and Drives (SDEMPED 2005)*, 2005, CD proceedings.
- [4] S. Rajagopalan, José A. Restrepo, José M. Aller, T. G. Habetler, and R. G. Harley, "Selecting Time-Frequency Representations for Detecting Rotor Faults in BLDC Motors Operating Under Rapidly Varying Operating Conditions," in *Proc. 32nd Annual Conference of the Industrial Electronics Society (IECON 2005)*, 2005, pp. 2579-2584.
- [5] Y. Zhao, L. E. Atlas, and R. J. Marks II, "The use of cone-shaped kernels for generalized time-frequency representations of nonstationary signals," *IEEE Trans. on Acoustics, Speech, and Signal Process.*, vol. 38, no. 7, pp. 1084-1091, 1990.
- [6] L. Cohen, "Generalized phase-space distribution functions," *J. Math. Phys.*, vol. 7, pp. 781-786, 1966.
- [7] L. Cohen and T. E. Posch, "Generalized ambiguity functions," in *Proc. IEEE International Conference on Acoustics, Speech, and Signal Processing, ICASSP '85*, 1985, pp. 1033-1036.
- [8] F. Auger, P. Flandrin, P. Goncalvès, and O. Lemoine, Time-frequency toolbox for use with MATLAB, CNRS France/Rice University, 1996.

- [9] D. L. Jones and R. G. Baraniuk, "An adaptive optimal-kernel time-frequency representation," *IEEE Trans. Signal Process.*, vol. 43, pp. 2361-2371, 1995.
- [10] F. Hlawatsch and G. F. Boudreaux-Bartels, "Linear and quadratic time-frequency representations," *IEEE Signal Processing Magazine*, pp. 21-67, 1992.
- [11] G. B. Kliman and J. Stein, "Methods of motor current signature analysis," *Electric Machines and Power Systems*, vol. 20, no. 5, pp. 463-474, 1992.
- [12] W. le Roux, S. Rajagopalan, R.G. Harley and T.G. Habetler, "On the detection of rotor faults in permanent magnet machines," in *Proc. Electric Machine Technology Symposium (EMTS 2004)*, 2004, CD-ROM.
- [13] B. Boashash, *Time-Frequency Signal Analysis – Methods and Applications*, Melbourne, Australia: Longman Cheshire, 1992, pp. 26.
- [14] B. Boashash and P. J. Black, "An efficient real-time implementation of the Wigner-Ville distribution," *IEEE Trans. on Acoustics, Speech, and Signal Process.*, vol. 35, no. 11, pp. 1611-1618, 1978.
- [15] F. Auger and P. Flandrin, "Improving the readability of time-frequency representation and time-scale representations by the reassignment method," *IEEE Trans. on Signal Process.*, vol.43, no. 5, pp. 1068-1089, 1995.